



## Reaction mechanisms of carbon dioxide capture by amino acid salt and desorption by heat or mineralization



Yiyi Li<sup>a,b</sup>, Xuelei Duan<sup>a</sup>, Weiguo Song<sup>b</sup>, Linge Ma<sup>a,\*</sup>, Jinder Jow<sup>a,\*</sup>

<sup>a</sup> National Institute of Clean-and-Low-Carbon Energy, Beijing 102211, China

<sup>b</sup> Beijing National Laboratory of Molecular Sciences, Institute of Chemistry, Chinese Academy of Science, Beijing 100190, China

### HIGHLIGHTS

- Both CO<sub>2</sub> absorption and desorption through the changes in carbamate and HCO<sub>3</sub><sup>-</sup>/CO<sub>3</sub><sup>2-</sup>.
- CO<sub>2</sub> desorption by mineralization higher than by heat due to low carbamate stability.
- A new mineralization mechanism for carbamate increasing with decreasing HCO<sub>3</sub><sup>-</sup>/CO<sub>3</sub><sup>2-</sup>.

### ARTICLE INFO

#### Keywords:

CO<sub>2</sub> capture  
Glycine  
Mineralization-desorption  
Chemical regeneration  
Quantitative nuclear magnetic resonance

### ABSTRACT

The reaction mechanisms of potassium glycine (KG)-CO<sub>2</sub> absorption, thermal desorption and mineralization desorption with CaO were studied based on the contents of carbamate, bicarbonate/carbonate, and KG/protonated KG analyzed by <sup>13</sup>C-quantitative nuclear magnetic resonance (<sup>13</sup>C qNMR). KG as the absorbent shows the CO<sub>2</sub> absorption efficiency up to 76% which has 57% due to the bicarbonate/carbonate formation and 43% due to the carbamate formation. Mineralization has a higher CO<sub>2</sub> desorption efficiency of 59% than that of thermal desorption (47%), and the results also indicate that carbamate is less stable under mineralization than under heat although both processes show the similar profiles as a function of pH value for carbamate and bicarbonate/carbonate. A new mechanism has been proposed to explain carbamate increasing with significantly decreasing bicarbonate/carbonate at the early stage of mineralization desorption while the other mechanisms reported in literatures have also been confirmed in this study.

### 1. Introduction

The increasing CO<sub>2</sub> emission has been reported to accelerate the global warming [1,2]. In order to deal with this global environmental problem, scientists have used many carbon-capture technologies to control the content of carbon dioxide in the atmosphere but there is nothing more quintessential than amine-based CO<sub>2</sub> capture [3–7]. The benchmark amine absorbent in industrial processes is mono-ethanol amine (MEA) [8]. But these kinds of alkanolamines generally have toxicity and volatility, especially when they undergo oxidative degradation in the flue gas resulting in the formation of undesirable by-products or difficult to reverse reactions [9]. On the other hand, the amino acid salts have some advantages over alkanolamines, such as environmental friendliness due to naturally occurring, low volatility due to their ionic structure and high surface tension, greater CO<sub>2</sub> absorption capacity than MEA, and high oxygen stability [9–16]. Several studies have used amino acid salts as absorbents in CO<sub>2</sub> capture and

investigated the reactions of amino acid salts with CO<sub>2</sub> [10–12,14,17–25]. However, the thermal regeneration energy of amino acid salts is generally higher than MEA in the CO<sub>2</sub>-absorption solution which means larger energy consumption needed for desorbing the same amount of CO<sub>2</sub> [26]. To deal with this problem, amino acid salt-based mineralization for absorbent regeneration has been explored to reduce the large energy consumption in the traditional thermal regeneration method [27]. In addition, the similar mineralization with Ca(OH)<sub>2</sub> has also been employed to regenerate amine successfully in different CO<sub>2</sub> absorption systems [28–32]. The integrated CO<sub>2</sub> absorption-mineralization process has great advantages in energy reduction and capital savings due to a larger cyclic CO<sub>2</sub> capacity, a requirement for less energy for absorbent desorption and no need for CO<sub>2</sub> compression and pipeline transport. This technology has great potential for industrial applications, particularly with CaO-containing industry wastes, such as high-CaO containing fly ash and other alkaline wastes [27,33,34].

In order to understand the process of amino acid salt-based CO<sub>2</sub>

\* Corresponding authors.

E-mail addresses: [linge.ma@chnenergy.com.cn](mailto:linge.ma@chnenergy.com.cn) (L. Ma), [jinde.zhuo@chnenergy.com.cn](mailto:jinde.zhuo@chnenergy.com.cn) (J. Jow).

capture mineralization-regeneration, it is necessary to study the reaction mechanism of the overall process. In the course of the CO<sub>2</sub>-capture studying, many methods, including NMR [9,35–51], Raman [52,53], FTIR [54–57] and XRD [33,34,58,59], have been used to investigate the interaction of the reactants. NMR techniques are widely used in qualitative and quantitative identification of chemical species. <sup>13</sup>C NMR spectroscopy is a suitable analytical method to get quantitative information on the species distribution in aqueous solutions loaded with CO<sub>2</sub>.

Some researchers have used <sup>13</sup>C NMR spectroscopy to qualitatively or quantitatively study the CO<sub>2</sub> absorption and desorption in alkanolamines and amino acid salts solutions [9,35–43,45–51]. The reaction mechanism can be derived from the changes which in the concentration of each substance during the whole process can be analyzed by <sup>13</sup>C NMR spectroscopy. However, up to date, especially in the amino acid salt solution, no study has been done to quantify the reaction mechanism of the CO<sub>2</sub> capture mineralization-regeneration process. There are numerical <sup>13</sup>C NMR studies to analyze the reaction products and establish the levels of all species in solution [9,35–43,45–51]. Hook et al. utilized <sup>13</sup>C NMR to find that amino acid salt solutions have better resistance to degradation. They indicated that the reactivity and CO<sub>2</sub> absorption capacity of amino acid salts are comparable to aqueous alkanolamines of related classes [9]. Hartono et al. studied aqueous solutions of diethylenetriamine (DETA) to absorb CO<sub>2</sub> at 298.0 K. From the loadings ranging from 0 to 1.69 by <sup>13</sup>C NMR, carbamate was one of the main species formed in the system at loadings below 1.0. At higher loadings (> 1.0), dicarbamate was dominated and HCO<sub>3</sub><sup>−</sup>/CO<sub>3</sub><sup>2−</sup> was also formed [42]. Then they performed qualitative <sup>13</sup>C NMR experiments at 298.0 K for different loadings to investigate the liquid speciation in amino acid neutralized by both strong inorganic and weak organic bases. They found the presence of carbamates from the amine groups of the primary and secondary amines as well as the amino acid even at very low loadings [41]. Zhang et al. used <sup>13</sup>C NMR for quantitative analysis on CO<sub>2</sub> absorption and desorption in the MEA solution. They found that the main species under the absorption conditions were free amine, protonated amine, MEA-based carbamate, and HCO<sub>3</sub><sup>−</sup>/CO<sub>3</sub><sup>2−</sup> [51]. Recently, Jing et al. used <sup>13</sup>C NMR to analyze the reaction intermediates under different CO<sub>2</sub> loadings and proposed mechanisms of CO<sub>2</sub> absorption and desorption in MEA [43]. Yu et al. used <sup>13</sup>C NMR to confirm the regeneration mechanism of MEA in mineralization [34]. The reaction mechanisms of CO<sub>2</sub> absorption by different types of amines and CO<sub>2</sub> desorption-amine regeneration via mineralization and thermal methods reported by literature are summarized below in Table 1 [27,33,34].

In our study, the reaction mechanism of carbon dioxide captured by an amino acid salt at 40 °C and CO<sub>2</sub> desorption via thermal method at 90 °C or mineralization by CaO at 25 °C will be derived by the concentration changes of key species, carbamate, amino acid/protonated amino acid, bicarbonate/carbonate, quantitatively measured by <sup>13</sup>C NMR spectroscopy. Glycine is chosen in this study due to its better CO<sub>2</sub>

absorption capability with non-toxic (environmentally friendly) and well-soluble in water (25 g/100 mL@25 °C) characterization, as well as suitable as an internal standard in the quantitative calculation of CO<sub>2</sub> loading because of its non-volatility and thermal stability. The percent conversions of two key chemical species, HCO<sub>3</sub><sup>−</sup>/CO<sub>3</sub><sup>2−</sup> and carbamate, can be easily quantified. Meanwhile, the whole reaction mechanisms of amino acid salt for CO<sub>2</sub> absorption as well as CO<sub>2</sub> desorption by thermal and mineralization methods can be proposed.

## 2. Materials and experimental method

### 2.1. Materials

Glycine (purity ≥ 99%) from Aladdin and calcium oxide (CaO, purity ≥ 99.95%) from Strem Chemicals were used. Potassium hydroxide KOH was purchased from Sinopharm. All of them were used without further purification. The amino acid salt solution, the potassium salt of glycine solution, H<sub>2</sub>NCH<sub>2</sub>COOK (KG), was prepared using equal molar amounts of potassium hydroxide KOH and glycine H<sub>2</sub>NCH<sub>2</sub>COOH (GY) in deionized water. Carbon dioxide (CO<sub>2</sub>, 99.995%) and nitrogen gases (N<sub>2</sub>, 99.99%) were purchased from BAPB Gases China.

### 2.2. Absorption-thermal or absorption-mineralization desorption experiment

The absorption-thermal desorption experiments were carried out in the reaction vessel in Fig. 1. The gas mixture with 15% CO<sub>2</sub> in N<sub>2</sub> was heated and bubbled through 150 mL aqueous KG solution (3 mol/L) in the bubble column at a flow rate of 1.5 L/min controlled by Sevenstar mass-flow controllers. The temperature of the column was maintained by a circulating oil bath at 40 °C during CO<sub>2</sub> absorption. The absorption temperature of 40 °C is selected to simulate the flue gas temperature. The CO<sub>2</sub> concentrations in the gas phase were recorded every 5 s using a Gasboard-3100P gas analyzer with its measurement range of 0–15 vol% CO<sub>2</sub>. The CO<sub>2</sub> bubbling in the KG solution was stopped when the CO<sub>2</sub> inlet concentration was equivalent to the CO<sub>2</sub> outlet concentration. The CO<sub>2</sub>-rich solution was obtained and regenerated in the same reaction vessel with oil bath at 90 °C. The thermal desorption was finished when the CO<sub>2</sub> outlet concentration was close to zero.

For the absorption-mineralization experiment, the CO<sub>2</sub>-rich solution (150 mL) was prepared the same as absorption-thermal desorption experiment and then transferred into a new reaction vessel (Fig. 2) with 0.45 mol CaO added for mineralization desorption. The mineralization desorption experiment was carried out in this reaction vessel. The pressure in the reaction vessel remained constant at atmospheric pressure throughout the experiment, and the temperature was maintained at 25 °C using a circulating oil bath. The CaO sample was well mixed with the CO<sub>2</sub>-rich solution by a magnetic stirrer at 500 rpm. The oil bath temperature was maintained at 25 °C during the mineralization

**Table 1**

The reaction mechanisms of CO<sub>2</sub> absorption by different types of amines and CO<sub>2</sub> desorption-amine regeneration via mineralization and thermal methods from literature.

Reaction step	Primary or Secondary amine	Sterically hindered or tertiary amines
amine solution	R <sub>1</sub> R <sub>2</sub> NH + H <sub>2</sub> O ⇌ R <sub>1</sub> R <sub>2</sub> NH <sub>2</sub> <sup>+</sup> + OH <sup>−</sup>	R <sub>1</sub> R <sub>2</sub> R <sub>3</sub> N + H <sub>2</sub> O ⇌ R <sub>1</sub> R <sub>2</sub> R <sub>3</sub> NH <sup>+</sup> + OH <sup>−</sup>
CO <sub>2</sub> absorption	2R <sub>1</sub> R <sub>2</sub> NH + CO <sub>2(aq)</sub> → R <sub>1</sub> R <sub>2</sub> NCOO <sup>−</sup> + R <sub>1</sub> R <sub>2</sub> NH <sub>2</sub> <sup>+</sup> CO <sub>2(aq)</sub> + OH <sup>−</sup> → HCO <sub>3</sub> <sup>−</sup> HCO <sub>3</sub> <sup>−</sup> ↔ CO <sub>3</sub> <sup>2−</sup> + H <sup>+</sup> R <sub>1</sub> R <sub>2</sub> NCOO <sup>−</sup> + H <sub>2</sub> O → R <sub>1</sub> R <sub>2</sub> NH + HCO <sub>3</sub> <sup>−</sup>	R <sub>1</sub> R <sub>2</sub> R <sub>3</sub> N + H <sub>2</sub> O + CO <sub>2(aq)</sub> → R <sub>1</sub> R <sub>2</sub> R <sub>3</sub> NH <sup>+</sup> + HCO <sub>3</sub> <sup>−</sup> CO <sub>2(aq)</sub> + OH <sup>−</sup> → HCO <sub>3</sub> <sup>−</sup> HCO <sub>3</sub> <sup>−</sup> ↔ CO <sub>3</sub> <sup>2−</sup> + H <sup>+</sup>
CO <sub>2</sub> thermal desorption and amine regeneration	HCO <sub>3</sub> <sup>−</sup> + R <sub>1</sub> R <sub>2</sub> NH <sub>3</sub> <sup>+</sup> <sup>heating</sup> → CO <sub>2</sub> ↑ + H <sub>2</sub> O + R <sub>1</sub> R <sub>2</sub> NH <sub>2</sub> CO <sub>3</sub> <sup>2−</sup> + 2R <sub>1</sub> R <sub>2</sub> NH <sub>3</sub> <sup>+</sup> <sup>heating</sup> → CO <sub>2</sub> ↑ + H <sub>2</sub> O + 2R <sub>1</sub> R <sub>2</sub> NH <sub>2</sub> R <sub>1</sub> R <sub>2</sub> NHCOO <sup>−</sup> + R <sub>1</sub> R <sub>2</sub> NH <sub>3</sub> <sup>+</sup> <sup>heating</sup> → 2R <sub>1</sub> R <sub>2</sub> NH <sub>2</sub> + CO <sub>2</sub> ↑	HCO <sub>3</sub> <sup>−</sup> + R <sub>1</sub> R <sub>2</sub> R <sub>3</sub> NH <sup>+</sup> <sup>heating</sup> → CO <sub>2</sub> ↑ + H <sub>2</sub> O + R <sub>1</sub> R <sub>2</sub> R <sub>3</sub> NCO <sub>3</sub> <sup>2−</sup> + 2R <sub>1</sub> R <sub>2</sub> R <sub>3</sub> NH <sup>+</sup> <sup>heating</sup> → CO <sub>2</sub> ↑ + H <sub>2</sub> O + 2R <sub>1</sub> R <sub>2</sub> R <sub>3</sub> N
CO <sub>2</sub> desorption by mineralization	CaO <sub>(s)</sub> + H <sub>2</sub> O → Ca <sup>2+</sup> + 2OH <sup>−</sup> Ca <sup>2+</sup> + OH <sup>−</sup> + HCO <sub>3</sub> <sup>−</sup> → CaCO <sub>3(s)</sub> + H <sub>2</sub> OR <sub>1</sub> R <sub>2</sub> NH <sub>2</sub> <sup>+</sup> + OH <sup>−</sup> ↔ R <sub>1</sub> R <sub>2</sub> NH + H <sub>2</sub> OR <sub>1</sub> R <sub>2</sub> NCOO <sup>−</sup> + H <sub>2</sub> O → R <sub>1</sub> R <sub>2</sub> NH + HCO <sub>3</sub> <sup>−</sup>	CaO <sub>(s)</sub> + H <sub>2</sub> O → Ca <sup>2+</sup> + 2OH <sup>−</sup> Ca <sup>2+</sup> + OH <sup>−</sup> + HCO <sub>3</sub> <sup>−</sup> → CaCO <sub>3(s)</sub> + H <sub>2</sub> OR <sub>1</sub> R <sub>2</sub> R <sub>3</sub> NH <sup>+</sup> + OH <sup>−</sup> ↔ R <sub>1</sub> R <sub>2</sub> R <sub>3</sub> N + H <sub>2</sub> O

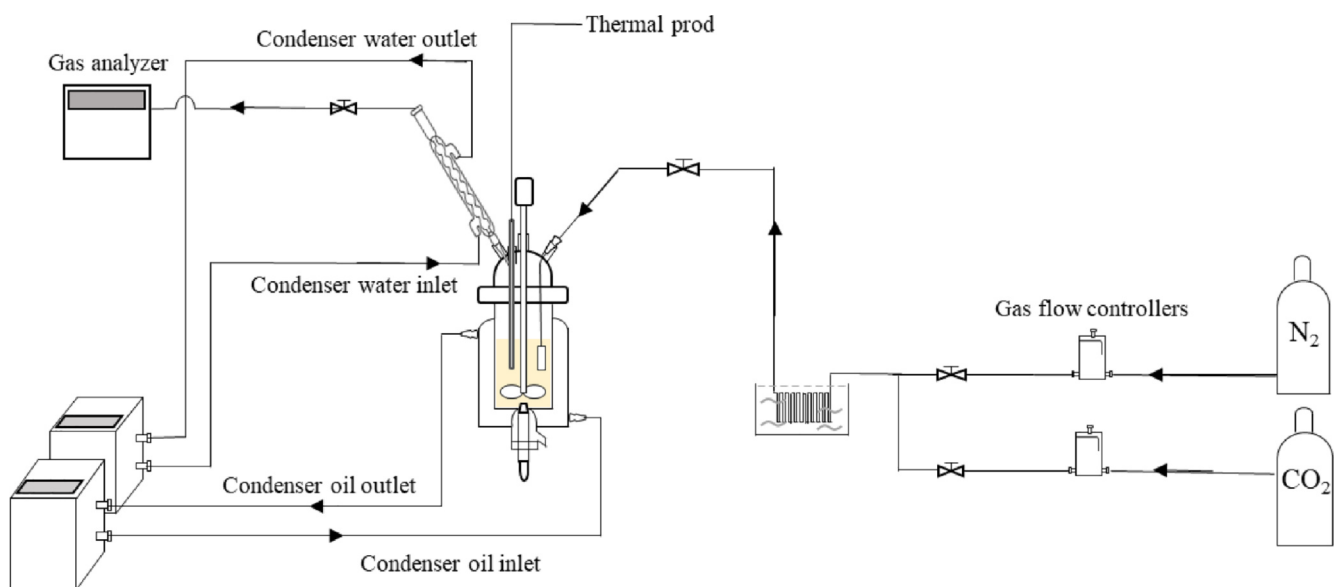


**Fig. 1.** Schematic diagram of CO<sub>2</sub> absorption-thermal desorption.

desorption so that the process did not produce thermal desorption due to heat release from the mineralization.

During the CO<sub>2</sub> absorption, thermal and mineralization desorption processes, the slurry samples (10 mL) were extracted with a syringe at selected time intervals, such as 3, 6, 9, 12, 15 and 18 min. The extracted solution was immediately filtered through a 0.2-μm nylon syringe filter for the mineralization experiment. Samples extracted from each experiment were used for pH value measurement and NMR analysis of key chemical species. The pH value was determined by pH meter from Mettler Toledo.

### 2.3. <sup>13</sup>C NMR spectra analysis

The NMR spectra were acquired at room temperature on an Avance III 400 MHz NMR spectrometer (Bruker) operating at the frequency of 100.62 MHz for <sup>13</sup>C and 400.13 MHz for <sup>1</sup>H. The experiment was conducted with the pulse program of zgig30 and a sweep width of 24038 Hz, using an acquisition time of 1.36 s and a relaxation delay (D1) of 50 s. The NMR samples were prepared with the same protocol, i.e. the sample solutions of 1000 μL were spiked with 50 μL of D<sub>2</sub>O (99.9 atom % D, Inno-Chem) in Wilmad quartz NMR tubes to get a signal lock, and NMR data were processed using the software of topspin 3.2.

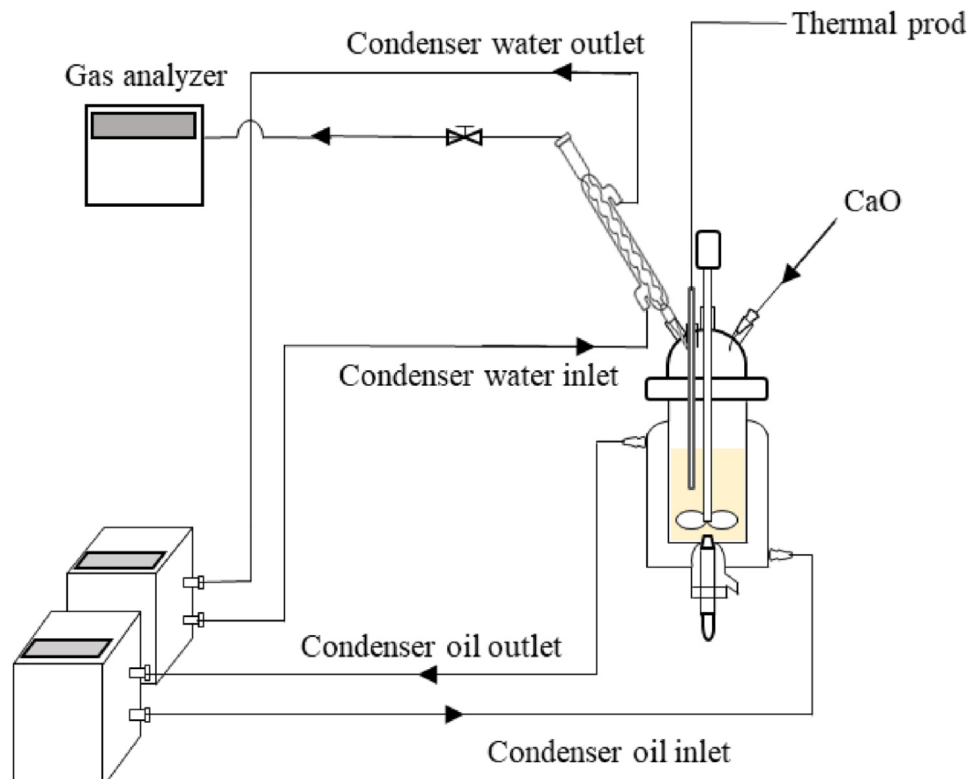


**Fig. 2.** Schematic diagram of mineralization desorption.

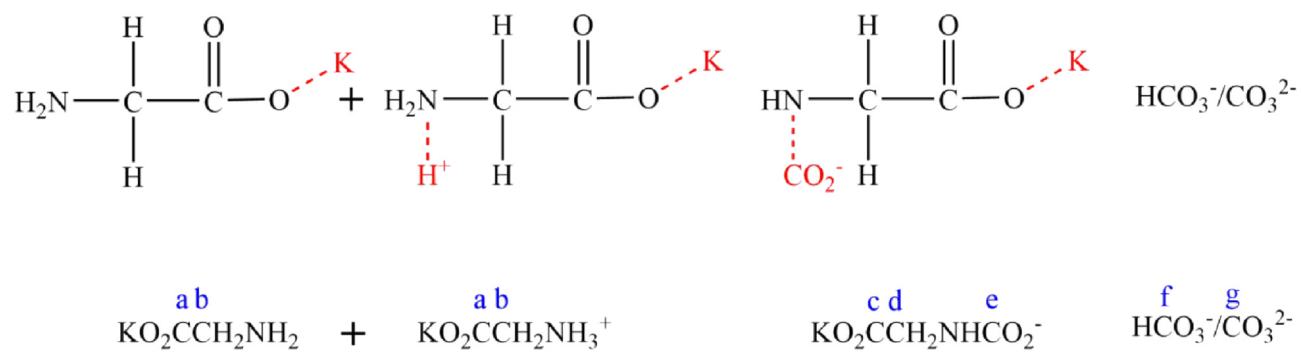


Fig. 3. Molecular structures and types of carbon nuclei in the KG system.

#### 2.4. Chemical system

The molecular structures of three key chemical species have different types of carbon nuclei visualized by the  $^{13}\text{C}$  NMR technique as shown in Fig. 3.

#### 3. Results and discussion

The aqueous KG solution was firstly prepared and equilibrated with  $\text{CO}_2$  absorption to quantitatively measure key carbon nuclei as shown in Fig. 3 by the  $^{13}\text{C}$  NMR spectroscopy. Then three types of experiments were conducted:  $\text{CO}_2$  absorption in the KG solution, thermal and mineralization desorption from the  $\text{CO}_2$ -rich KG solution. The  $^{13}\text{C}$  NMR spectra data and pH values of experimental samples taken at selected times during each experiment were measured and recorded.

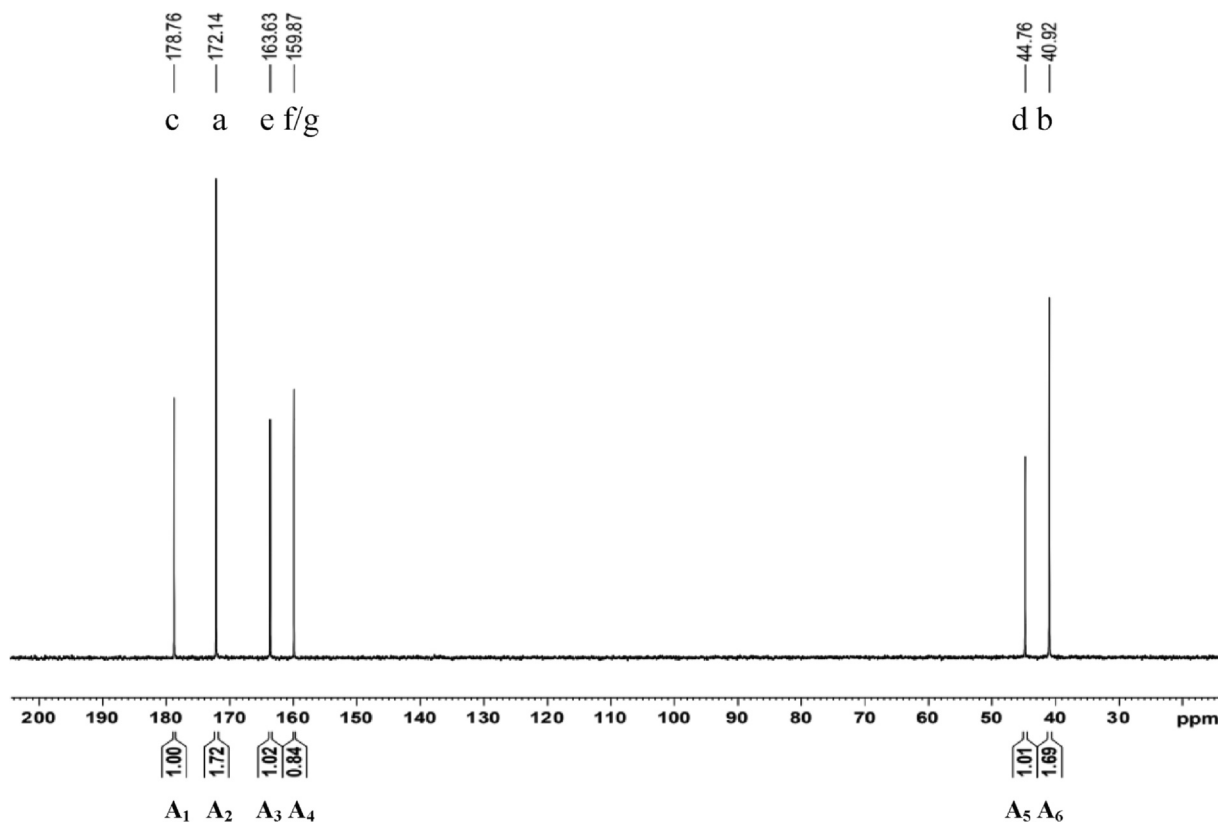
##### 3.1. Quantification calculation with $^{13}\text{C}$ NMR spectrum

The aqueous KG solution equilibrated with  $\text{CO}_2$  absorption was

**Table 2**  
Peak Assignment and Integration Area of one  $\text{CO}_2$ -loading Samples.

No.	$\delta/\text{ppm}$	Assignment	Integration Area	Related compounds
1	178.76	$-\text{CH}_2-\text{C}(=\text{O})-$	A <sub>1</sub>	$\text{KO}_2\text{CCH}_2\text{NHCO}_2^-$
2	172.14	$-\text{C}(=\text{O})-$	A <sub>2</sub>	$\text{KO}_2\text{CCH}_2\text{NH}_2/\text{KO}_2\text{CCH}_2\text{NH}_3^+$
3	163.63	$-\text{NH}-\text{C}(=\text{O})-$	A <sub>3</sub>	$\text{KO}_2\text{CCH}_2\text{NHCO}_2^-$
4	159.87	$\text{HCO}_3^-/\text{CO}_3^{2-}$	A <sub>4</sub>	Bicarbonate/Carbonate
5	44.76	$-\text{CH}_2-$	A <sub>5</sub>	$\text{KO}_2\text{CCH}_2\text{NHCO}_2^-$
6	40.92	$-\text{CH}_2-$	A <sub>6</sub>	$\text{KO}_2\text{CCH}_2\text{NH}_2/\text{KO}_2\text{CCH}_2\text{NH}_3^+$

prepared and measured by the  $^{13}\text{C}$  NMR spectroscopy. The  $^{13}\text{C}$  NMR spectra results were obtained as shown in Fig. 4. The signal, its structure and integration area, and related compound are listed in Table 2. The presences of  $\text{KO}_2\text{CCH}_2\text{NH}_2/\text{KO}_2\text{CCH}_2\text{NH}_3^+$  (potassium glycine KG/protonated potassium glycine KGH $^+$ ),  $\text{KO}_2\text{CCH}_2\text{NHCO}_2^-$  (carbamate), and  $\text{HCO}_3^-/\text{CO}_3^{2-}$  (bicarbonate/carbonate), were observed. The signal

Fig. 4.  $^{13}\text{C}$  NMR spectrum of one sample from the absorption.

of 163.63 ppm (e in Fig. 3) shows the presence of carbamate ( $A_3$ ), and the other two carbon signals of carbamate ( $A_1$  and  $A_5$ ) were located at 178.76 and 44.76 ppm (c and d in Fig. 3), respectively. The peaks of 172.14 and 40.92 ppm (a and b in Fig. 3) were assigned as carbonyl group and methylene group in the KG/KGH<sup>+</sup> ( $A_2$  and  $A_6$ ). The position of the peak at 159.87 ppm (f or g in Fig. 3) indicates that the existence of bicarbonate or carbonate ( $A_4$ ).

As the quantitative NMR spectrum is shown in Fig. 4, the integration area of  $A_1$ ,  $A_3$  and  $A_5$  should be the same in theory, representing carbamate, while  $A_2$  also equals to  $A_6$ , representing both KG and protonated KG.  $A_4$  represents bicarbonate/carbonate. Therefore, only integration areas of  $A_1$ ,  $A_2$ , and  $A_4$  are chosen to represent the contents of 3 key chemical species for the subsequent calculation. Since  $A_1$  was used as the internal standard, the value of  $A_1$  was calibrated as 1.00 to relatively calculate the values of  $A_2$  and  $A_3$ , and  $A_4$  based on the integration results of <sup>13</sup>C NMR Spectra. The average value of  $A_3$  is  $1.01 \pm 0.01$ . This confirms  $A_3$  statistically equal to  $A_1$ , and good accuracy in the NMR spectra measurement, assuming the normal distribution for NMR data. The sum  $A_1$  and  $A_2$  represents the initial content of potassium glycine (KG). The sum of  $A_1$  and  $A_4$  represents the contents of CO<sub>2</sub> loading (from carbamate and bicarbonate/carbonate). On the basis of the peak assignment and integration area, the values of these three key contents can be calculated by the following equations 1–3:

$$\text{Carbamate content ((mol/mol Glycine)} = A_1/(A_1 + A_2) \quad (1)$$

$$\text{Bicarbonate/Carbonate content (mol/mol Glycine)} = A_4/(A_1 + A_2) \quad (2)$$

$$\text{CO}_2 \text{ loading content (mol/mol Glycine)} = (A_1 + A_4)/(A_1 + A_2) \quad (3)$$

As glycine always exists as KG/KGH<sup>+</sup> and carbamate since the introduction of CO<sub>2</sub>, the sum of  $A_1$  and  $A_2$  are normalized as 1 in order to see the relative changes of these two species under different pH values. The contents of carbamate, bicarbonate/carbonate, and CO<sub>2</sub> loading are then calculated according to Equations 1 to 3, respectively (see Tables 3–8), as functions of the pH values during CO<sub>2</sub> absorption and desorption. The results of <sup>13</sup>C NMR Spectra for the CO<sub>2</sub> absorption experiment are shown in Figs. 5–7.

### 3.2. <sup>13</sup>C NMR spectra results of CO<sub>2</sub> absorption into the KG solution

The <sup>13</sup>C NMR Spectra under different pH values during CO<sub>2</sub> absorption in the KG solution are shown in Fig. 5. The <sup>13</sup>C NMR spectra data and pH values of the experimental samples taken out during the CO<sub>2</sub> absorption in the KG solution were measured.

Since  $A_1$  used as the internal standard has its integration area of 1.00,  $A_2$ , and  $A_3$ , and  $A_4$  are measured relative to  $A_1$  based on the <sup>13</sup>C NMR Spectra data in Fig. 5. The results are listed in Table 3 of the absorption experiment. For both batches, the average value of  $A_3$  is  $1.01 \pm 0.01$  with 3 standard deviations of 0.04. This confirms  $A_3$  statistically equal to  $A_1$ , and good accuracy in the NMR spectra measurement, assuming the normal distribution for NMR data.

Based on the principle of mass conservation, the sum of  $A_1$  and  $A_2$

**Table 3**  
<sup>13</sup>C NMR and pH data for samples from CO<sub>2</sub> absorption.

Sample No.	A <sub>1</sub> Reference	A <sub>2</sub>	A <sub>3</sub>	A <sub>4</sub>	pH Value
1	—	—	—	—	13.93
2	1.00	2.15	1.01	0.05	11.52
3	1.00	1.17	1.01	0.21	10.02
4	1.00	1.36	1.02	0.42	9.61
5	1.00	1.60	1.02	0.73	9.16
6	1.00	1.77	0.98	0.94	8.91
7	1.00	2.07	1.00	1.31	8.40

**Table 4**  
pH, Carbamate, KG/KGH<sup>+</sup>, HCO<sub>3</sub><sup>-</sup>/CO<sub>3</sub><sup>2-</sup>, CO<sub>2</sub> loading data for CO<sub>2</sub> absorption.

Contents	Carbamate	KG/KGH <sup>+</sup>	HCO <sub>3</sub> <sup>-</sup> /CO <sub>3</sub> <sup>2-</sup>	CO <sub>2</sub> loading
pH Value	A <sub>1</sub> /(A <sub>1</sub> + A <sub>2</sub> )	A <sub>2</sub> /(A <sub>1</sub> + A <sub>2</sub> )	A <sub>4</sub> /(A <sub>1</sub> + A <sub>2</sub> )	(A <sub>1</sub> + A <sub>4</sub> )/(A <sub>1</sub> + A <sub>2</sub> )
13.93	0.00	1.00	0.00	0.00
11.52	0.32	0.68	0.02	0.34
10.02	0.46	0.54	0.10	0.56
9.61	0.42	0.58	0.18	0.60
9.16	0.38	0.62	0.28	0.66
8.91	0.36	0.64	0.34	0.70
8.40	0.33	0.67	0.43	0.76

**Table 5**  
<sup>13</sup>C NMR spectra of CO<sub>2</sub> desorption by heat at various pH.

Sample No.	A <sub>1</sub> reference	A <sub>2</sub>	A <sub>3</sub>	A <sub>4</sub>	pH Value
1	1.00	1.74	1.03	0.83	8.60
2	1.00	1.12	0.98	0.22	9.08
3	1.00	1.18	1.03	0.26	9.38
4	1.00	1.12	1.00	0.18	9.67
5	1.00	1.13	1.01	0.08	10.07
6	1.00	1.40	1.02	0.07	10.80
7	1.00	2.05	1.01	0.05	11.07

**Table 6**  
<sup>13</sup>C NMR spectra and pH data for CO<sub>2</sub> desorption by heat.

Contents	Carbamate	KG/KGH <sup>+</sup>	HCO <sub>3</sub> <sup>-</sup> /CO <sub>3</sub> <sup>2-</sup>	CO <sub>2</sub> loading
pH Value	A <sub>1</sub> /(A <sub>1</sub> + A <sub>2</sub> )	A <sub>2</sub> /(A <sub>1</sub> + A <sub>2</sub> )	A <sub>4</sub> /(A <sub>1</sub> + A <sub>2</sub> )	(A <sub>1</sub> + A <sub>4</sub> )/(A <sub>1</sub> + A <sub>2</sub> )
8.60	0.36	0.64	0.30	0.66
9.08	0.47	0.53	0.10	0.57
9.38	0.46	0.54	0.12	0.58
9.67	0.47	0.53	0.08	0.55
10.37	0.47	0.53	0.04	0.51
10.80	0.42	0.58	0.03	0.45
11.07	0.33	0.67	0.02	0.35

**Table 7**  
<sup>13</sup>C NMR spectra and pH data for CO<sub>2</sub> desorption by mineralization.

Sample No.	A <sub>1</sub> reference	A <sub>2</sub>	A <sub>3</sub>	A <sub>4</sub>	pH Value
1	1.00	1.72	1.02	0.84	8.60
2	1.00	1.56	0.95	0.73	8.63
3	1.00	1.41	0.98	0.51	8.83
4	1.00	1.20	0.99	0.27	9.28
5	1.00	1.12	1.02	0.15	9.80
6	1.00	1.42	1.01	0.06	10.30
7	1.00	2.66	1.00	0.05	10.97

**Table 8**  
pH, Carbamate, KG/KGH<sup>+</sup>, HCO<sub>3</sub><sup>-</sup>/CO<sub>3</sub><sup>2-</sup>, CO<sub>2</sub> loading under mineralization.

Contents	Carbamate	KG/KGH <sup>+</sup>	HCO <sub>3</sub> <sup>-</sup> /CO <sub>3</sub> <sup>2-</sup>	CO <sub>2</sub> loading
pH Value	A <sub>1</sub> /(A <sub>1</sub> + A <sub>2</sub> )	A <sub>2</sub> /(A <sub>1</sub> + A <sub>2</sub> )	A <sub>4</sub> /(A <sub>1</sub> + A <sub>2</sub> )	(A <sub>1</sub> + A <sub>4</sub> )/(A <sub>1</sub> + A <sub>2</sub> )
8.60	0.37	0.63	0.31	0.68
8.63	0.39	0.61	0.29	0.68
8.83	0.41	0.59	0.21	0.62
9.28	0.45	0.55	0.12	0.57
9.80	0.47	0.53	0.07	0.54
10.3	0.41	0.59	0.02	0.43
10.97	0.27	0.73	0.01	0.28

should be always the same for each sample taken out from the experiment run. Including the obvious initial data at high pH values before CO<sub>2</sub> introduction, we can re-ratio A<sub>1</sub> and A<sub>2</sub> and re-calculate A<sub>3</sub> and A<sub>4</sub> to generate carbamate, KG/KGH<sup>+</sup>, HCO<sub>3</sub><sup>-</sup>/CO<sub>3</sub><sup>2-</sup>, CO<sub>2</sub> loading data in Table 4 listed below.

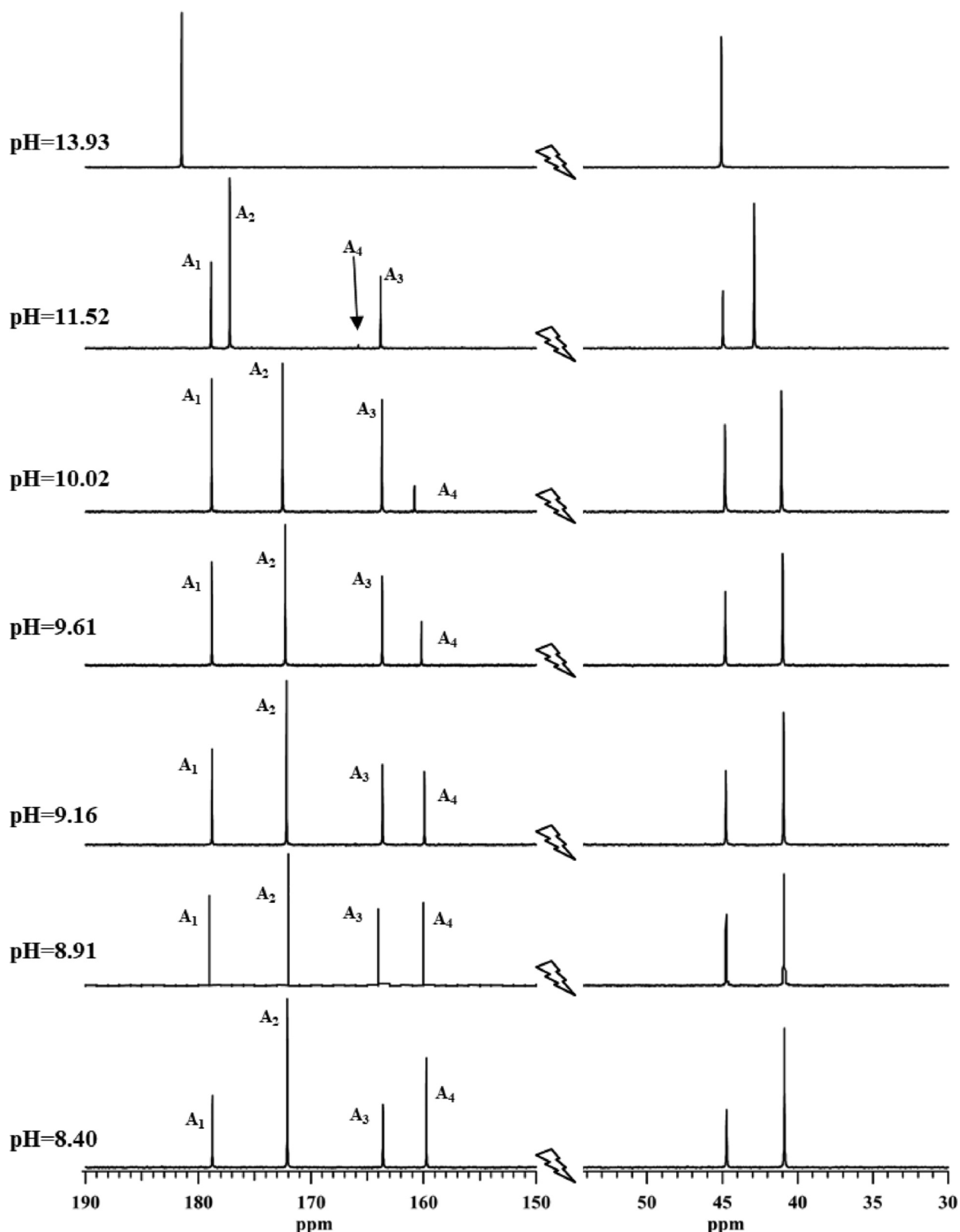


Fig. 5.  $^{13}\text{C}$  NMR spectra of  $\text{CO}_2$  absorption into KG Solution.

### 3.3. $^{13}\text{C}$ NMR spectra results of thermal desorption from the $\text{CO}_2$ -rich KG solution

The  $^{13}\text{C}$  NMR Spectra under different pH values during thermal regeneration from  $\text{CO}_2$ -rich KG Solution are shown in Fig. 6. The  $^{13}\text{C}$

NMR spectra data and pH values of the experimental samples taken out during thermal desorption from the  $\text{CO}_2$ -rich KG solution were obtained.

Again, A<sub>1</sub> used as the internal standard has the integration area of 1.00. A<sub>2</sub>, and A<sub>3</sub>, and A<sub>4</sub> are measured relative to A<sub>1</sub> based on the  $^{13}\text{C}$

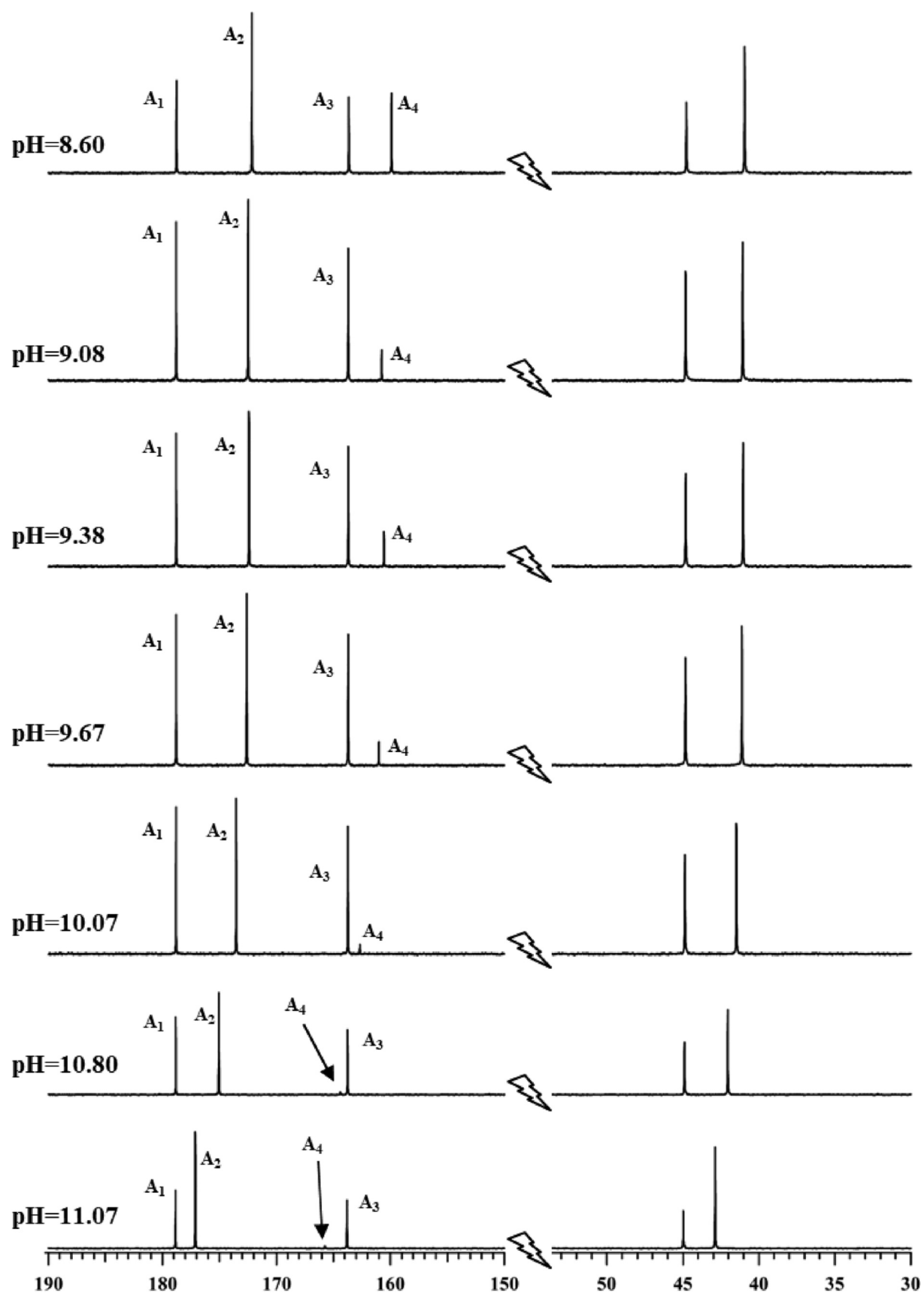
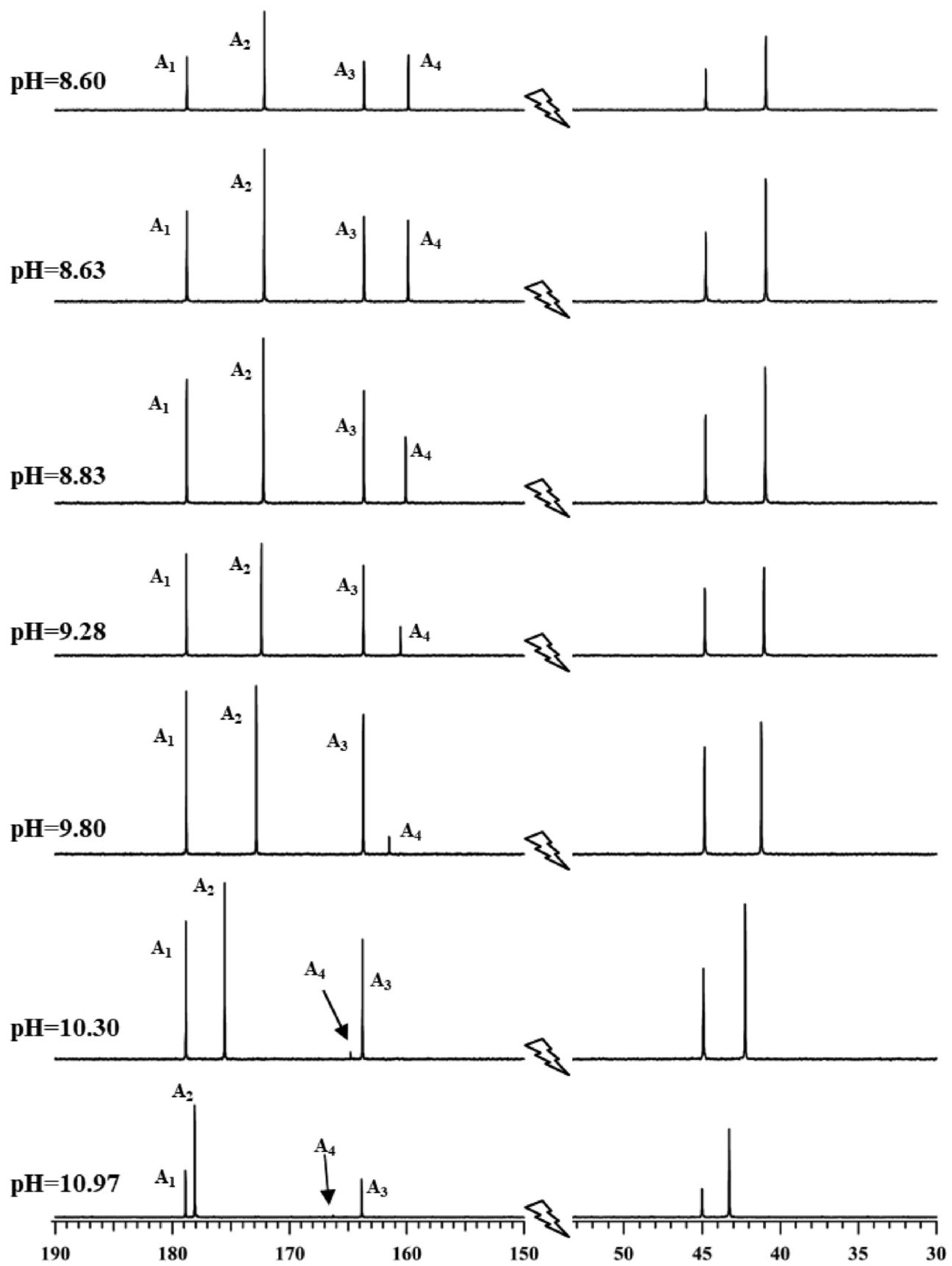


Fig. 6.  $^{13}\text{C}$  NMR spectra of thermal regeneration from  $\text{CO}_2$ -rich KG Solution.

Fig. 7.  $^{13}\text{C}$  NMR spectra of mineralization from  $\text{CO}_2$ -rich KG Solution.

NMR Spectra data in Fig. 6. The results are listed in Table 5. The average value of  $A_3$  in two batches is  $1.01 \pm 0.02$  with 3 standard deviations of 0.05.  $A_3$  statistically equals to  $A_1$ .

Since the sum of  $A_1$  and  $A_2$  should be always the same, we can re-ratio  $A_1$  and  $A_2$  and re-calculate  $A_3$  and  $A_4$  in Table 5 to generate carbamate,  $\text{KG}/\text{KGH}^+$ ,  $\text{HCO}_3^-/\text{CO}_3^{2-}$ ,  $\text{CO}_2$  loading at each pH value listed in Table 6.

### 3.4. $^{13}\text{C}$ NMR spectra results of mineralization from the $\text{CO}_2$ -rich KG solution

The  $^{13}\text{C}$  NMR Spectra under different pH values during mineralization from  $\text{CO}_2$ -rich KG Solution are shown in Fig. 7. The  $^{13}\text{C}$  NMR spectra data and pH values of the experimental samples taken out during mineralization from the  $\text{CO}_2$ -rich KG solution were measured.

Again,  $A_1$  used as the internal standard has the value of 1.00.  $A_2$ , and  $A_3$ , and  $A_4$  are measured relative to  $A_1$  based on the  $^{13}\text{C}$  NMR Spectra data in Fig. 7. The results are listed in Table 7. The average value of  $A_3$  is  $1.00 \pm 0.02$  with 3 standard deviations of 0.07. Apparently,  $A_3$  statistically equals to  $A_1$ .

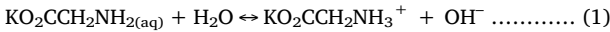
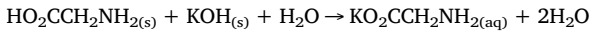
Since the sum of  $A_1$  and  $A_2$  should be always the same, we can re-ratio  $A_1$  and  $A_2$  and re-calculate  $A_3$  and  $A_4$  in Table 7 to calculate the contents of carbamate,  $\text{KG}/\text{KGH}^+$ ,  $\text{HCO}_3^-/\text{CO}_3^{2-}$ ,  $\text{CO}_2$  loading as listed in Table 8.

### 3.5. $\text{CO}_2$ absorption and desorption by heat

The pH values were measured and  $^{13}\text{C}$  qNMR experiments were conducted for the samples taken out during the  $\text{CO}_2$  absorption in the KG solution and desorption by heat. The results are shown in Fig. 8 (A) for absorption and (B) for desorption by heat.

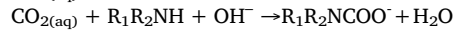
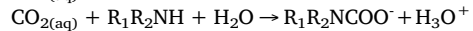
#### 3.5.1. $\text{CO}_2$ absorption

The starting aqueous KG solution is in equilibrium as described by the mechanism as below. The NMR spectrum of pH = 13.93 has only the presence of  $\text{KO}_2\text{CCH}_2\text{NH}_2$  (KG) and  $\text{KO}_2\text{CCH}_2\text{NH}_3^+$  ( $\text{KGH}^+$ ) as the first data point shown in Fig. 5.

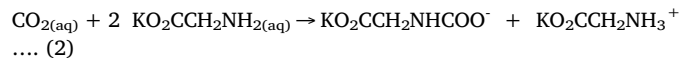


With the introduction of  $\text{CO}_2$  to the starting solution, carbamate ( $\text{KO}_2\text{CCH}_2\text{NHCOO}^-$ ) was formed firstly where no bicarbonate/carbonate was formed, then its content decreases after reaching its maximum, while the content of bicarbonate/carbonate was slightly increased at first, then significantly increased more than the reduction in

carbamate as the pH value was continuously decreased. At the end of the  $\text{CO}_2$  absorption, the formation of bicarbonate/carbonate contributes more to  $\text{CO}_2$  loading than the carbamate formation. There are three possible primary/secondary amine-based routes for the carbamate formation reported in literature through the zwitterionic mechanism as listed below [20,60–62]. The first one is widely accepted.



To explain the early increase in carbamate formation (0 to 0.32 mol/mol) with the same amount in the  $\text{KG}/\text{KGH}^+$  reduction (1.00 to 0.68 mol/mol) under no or very low increase in the bicarbonate/carbonate formation (0.00 to 0.02 mol/mol) for the pH value of 13.93 decreased to 11.52, the first proposed mechanism is the absorbed 1 mol  $\text{CO}_2$  reacting with 2 mol KG to produce 1 mol carbamate and 1 mol protonated KG ( $\text{KGH}^+$ ) as described below (2). More protonated KG formation results in a lower pH value.



The content of carbamate increased continuously with the decreasing in pH as the continuous introduction of  $\text{CO}_2$ . The content of bicarbonate/carbonate increased from 0.02 to 0.10 mol/mol, but its increment was lower than that of carbamate increased from 0.32 to 0.46 mol/mol as the pH value was reduced from 11.52 to 10.02 listed in Table 4. This suggests the above mechanism is still going on and more than the well-known mechanisms (3 and 4) for bicarbonate formation, instead of carbonic acid formation which is very slow and can be neglected  $\text{CO}_{2(aq)} + \text{H}_2\text{O} \rightarrow \text{H}^+ + \text{HCO}_3^-$ , and bicarbonate in equilibrium with carbonate as described, respectively.



After the carbamate content reached its maximum value of 0.46 mol/mol KG, the bicarbonate/carbonate content showed a stronger increase but the carbamate content was declined with the same amount of  $\text{KG}/\text{KGH}^+$  increase. This suggests that mechanism (2) has stopped. A new mechanism was started. As the pH value of 10.02 was reduced to 9.61, the bicarbonate/carbonate was increased from 0.10 to 0.18 mol/mol but the carbamate content was decreased from 0.46 to 0.42 mol/mol with the same amount of  $\text{KG}/\text{KGH}^+$  increased from 0.54 to 0.58 mol/mol. This new mechanism is described below by consuming carbamate to produce bicarbonate as well as regenerate KG. It has been reported in literature [43].

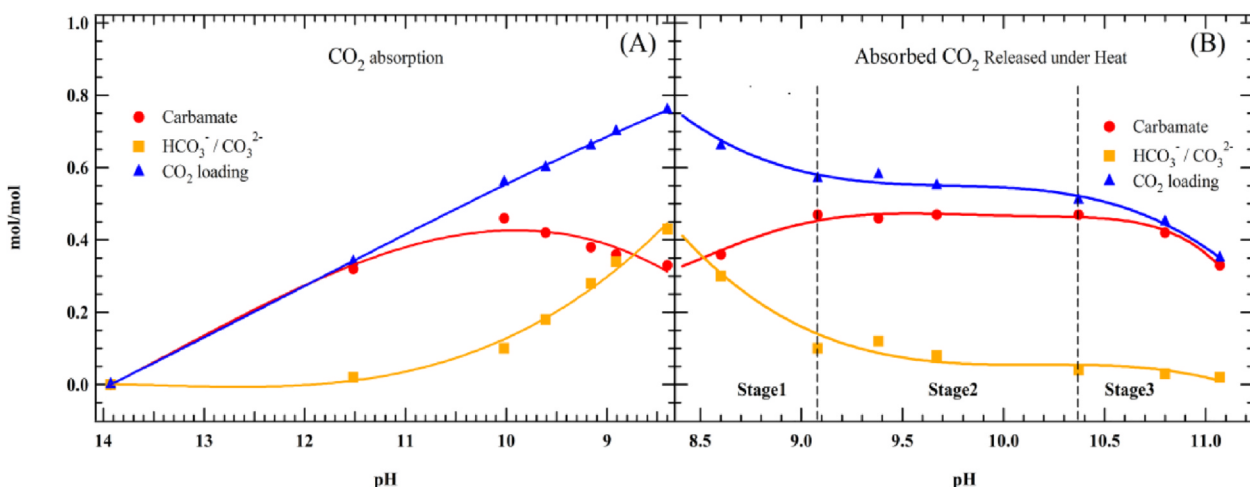


Fig. 8. Carbamate,  $\text{HCO}_3^-/\text{CO}_3^{2-}$ ,  $\text{CO}_2$  loading vs pH for  $\text{CO}_2$  absorption and desorption by heat.



The content of carbamate was continuously decreased with the decreasing in pH value, while bicarbonate/carbonate was continuously increased. The content of bicarbonate/carbonate was significantly increased, much higher than the reduction in carbamate with the same amount of KG regeneration, indicating that mechanisms (3) and (5) co-exist at the pH values from 9.61 down to 8.40. At the end of the experiment, carbamate, bicarbonate/carbonate and KG/KGH<sup>+</sup> were all in the equilibrium.

Overall, the CO<sub>2</sub> loading at the beginning was due to the carbamate formation and continuously increased, dominated by the carbamate formation as the decrease in pH value with a very low bicarbonate/carbonate formation. As the carbamate content reached its maximum, bicarbonate/carbonate was significantly increased as the dominated mechanism. After carbamate reached its maximum and was decreased in the amount less than the increase in bicarbonate/carbonate. Apparently, the key contribution to the CO<sub>2</sub> loading was shifted from carbamate formation to bicarbonate/carbonate formation. The final reduction in carbamate also helped the increase in bicarbonate/carbonate formation. The reaction mechanisms for CO<sub>2</sub> absorption in the KG solution proposed in this study are similar to those reported in literature [27,33,34].

At the final pH value of 8.40 as listed in Table 4, the CO<sub>2</sub> loading level reached to 0.76 mol/mol KG with 0.33 mol/mol KG from carbamate and 0.43 mol/mol KG from bicarbonate/carbonate. This means that the CO<sub>2</sub> absorption efficiency is about 76% with 0.33% (43%) from carbamate and 0.43% (57%) from bicarbonate/carbonate.

### 3.5.2. CO<sub>2</sub> desorption by heat

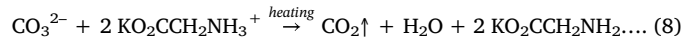
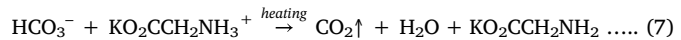
The contents of carbamate, bicarbonate/carbonate, and CO<sub>2</sub> loading as functions of the pH values during the thermal desorption are shown in Fig. 8(B) based on data listed in Table 6. It clearly indicates three different stages. Stage 1 has the increase in carbamate but much significant decrease in bicarbonate/carbonate as the pH value was increasing. Stage 2 has the carbamate reaching its maximum and remaining relatively constant as the pH value is continuously increased, and the slower reduction in bicarbonate/carbonate content. Stage 3 has the reduction in carbamate higher than the reduction in bicarbonate/carbonate. Based on the initial to the final data for the thermal desorption at 90 °C, the results suggest that the significant reduction in bicarbonate/carbonate content was the primary factor for CO<sub>2</sub> desorption, even though the carbamate reduction is dominated at the end of thermal desorption but the final content was only slightly lower than its initial content.

Stage 1: From the initial increase in the pH value from 8.60 to 9.08, an increase in the carbamate content from 0.36 to 0.47 mol/mol, simultaneously, a more significant decrease in the bicarbonate/carbonate content were observed from 0.30 to 0.10 mol/mol. The CO<sub>2</sub> loading was decreased due to loss of 2 mol bicarbonates with only 1 mol increase in carbamate. Therefore, the first thermal degradation mechanism (6) is proposed to have 2 mol bicarbonates reacting with 1 mol protonated KG to generate 1 mol carbamate molecule and release 1 mol CO<sub>2</sub> as described below.

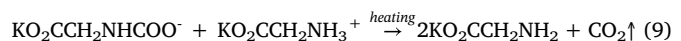


Stage 2: As the pH value was further increased from 9.08 to 10.37, the carbamate content reached its maximum but remained relatively constant at about 0.46–0.47 mol/mol, and the bicarbonate/carbonate content was continuously reduced from 0.10 to 0.04 mol/mol. This suggests that mechanism (6) has been stopped and bicarbonate/carbonate reacting with protonated KG were thermally degraded to produce CO<sub>2</sub> and regenerate KG as the primary mechanisms described by

mechanisms (7) and (8) as described below. Both have been reported in literature. These two mechanisms show how Protonated KG can be regenerated back to KG.



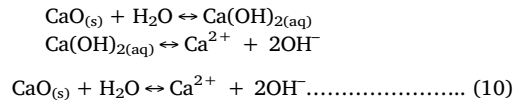
Stage 3: As the pH value was continuously increased from 10.37 to 10.80, the carbamate decreased from 0.47 to 0.42 mol/mol, while the bicarbonate/carbonate content was reduced very little from 0.04 to 0.03 mol/mol or remained relatively constant at a very low level. This further reduction in the CO<sub>2</sub> loading was primarily due to carbamate reacting with protonated KG under heat to regenerate KG and CO<sub>2</sub>. Below is the proposed mechanism (9) which has been also reported in literature. Protonated KG is also regenerated back to KG through this mechanism. The same was also applied when the pH value was increased from 10.80 to 11.07; the reduction in carbamate from 0.42 to 0.33 mol/mol results in increasing the same mole of KG/KGH<sup>+</sup> from 0.58 to 0.67 mol/mol and releasing the same mole of CO<sub>2</sub> by mechanism (9).



At the pH value of 8.60 increased to 11.07 for this thermal desorption experiment at 90 °C, the CO<sub>2</sub> loading of 0.67 mol/mol KG (0.36 mol/mol from carbamate and 0.30 mol/mol from bicarbonate/carbonate) was decreased to 0.34 mol/mol KG (0.33 mol/mol from carbamate and 0.02 mol/mol from bicarbonate/carbonate). The overall CO<sub>2</sub> desorption efficiency is 49% with 45% (91%) from bicarbonate/carbonate and 4% (9%) from carbamate by the thermal method at 90 °C in the CO<sub>2</sub>-rich KG solution. This suggests that heat is much easier to release CO<sub>2</sub> from bicarbonate/carbonate than from carbamate.

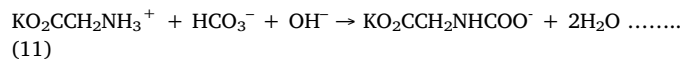
### 3.6. CO<sub>2</sub> desorption by mineralization

The following mechanisms are typically used to describe the addition of CaO into the CO<sub>2</sub>-rich KG solution as shown below (10).



The CO<sub>2</sub> loading, the carbamate and bicarbonate/carbonate loading as functions of pH values during mineralization from the CO<sub>2</sub>-rich KG solution are shown in Fig. 9 based on Table 8. Apparently, we observed the profiles of carbamate and bicarbonate/carbonate similar to those in thermal desorption. The increase in carbamate was about half of the reduction in bicarbonate/carbonate before the carbamate reached its maximum. After the carbamate reached its maximum, carbamate was reduced, while the bicarbonate/carbonate content was also reduced and stabilized at a very low level as the pH value was further increased to the end of mineralization desorption.

As the pH value was increased from 8.60 to 8.83, the reduction in bicarbonate/carbonate was significantly (from 0.31 to 0.21 mol/mol KG) about twice of the increase in carbamate formation (from 0.37 to 0.41 mol/mol KG), resulting in decreasing the CO<sub>2</sub> loading from 0.68 to 0.62 mol/mol KG. A new mechanism (11) is proposed to explain the increase in carbamate, while the reduction in bicarbonate/carbonate, which has not been reported in literature.



Of course, the most common well-known carbonation mechanism explains the additional decrease in carbonate as described below (12).

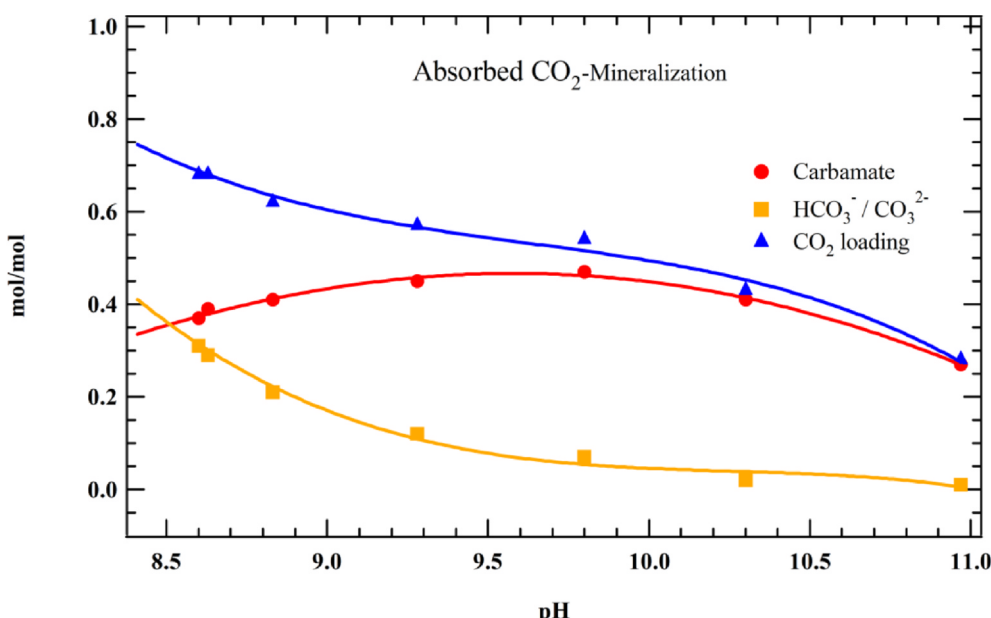
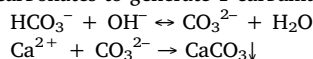


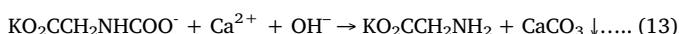
Fig. 9. Carbamate, HCO<sub>3</sub><sup>-</sup>/CO<sub>3</sub><sup>2-</sup>, CO<sub>2</sub> loading vs pH for absorbed CO<sub>2</sub> release by mineralization.

Both mechanisms were at the same rate to support consumption of 2 bicarbonates to generate 1 carbamate.



From the pH value of 8.83 increased to 9.28, the carbamate content was increased from 0.41 to 0.45 mol/mol and the bicarbonate/carbonate was decreased from 0.21 to 0.12 mol/mol KG. The same mechanisms as the above were also applied. From the pH value of 9.28 increased to 9.80, the carbamate content was increased from 0.45 to 0.47 mol/mol and the bicarbonate/carbonate was decreased from 0.12 to 0.07 mol/mol KG. Both mechanisms (11) and (12) were still at the same rate.

From the pH value of 9.80 increased to 10.97, the carbamate content was further decreased from 0.47 to 0.27 mol/mol and the bicarbonate/carbonate was also decreased from 0.07 to 0.01 mol/mol. The reduction in the bicarbonate/carbonate content was still explained by the previous mechanism (12). But mechanism (11) was stopped. Instead, the reduction in carbamate could be explained by consuming carbamate by reacting with Ca<sup>2+</sup> to regenerate the same mole of KG and produce the same mole of precipitated CaCO<sub>3</sub> as described by the mechanism (13) below.



For mineralization with CaO at 25 °C, the reduction in CO<sub>2</sub> loading was driven by Ca<sup>2+</sup> reacting with bicarbonate/carbonate through carbonation as well as with carbamate through absorbent regeneration. The results show the CO<sub>2</sub> desorption efficiency about 59%, slightly higher than the thermal method, and have 75% contributed from bicarbonate/carbonate and 25% from carbamate. This also suggests that mineralization is much easier to release CO<sub>2</sub> from bicarbonate/carbonate than that from carbamate, and much easier than the thermal method.

### 3.7. CO<sub>2</sub> absorption and desorption efficiency and mechanisms

Key findings of the carbamate, bicarbonate/carbonate, and CO<sub>2</sub> loading at various pH values for CO<sub>2</sub> absorption at 40 °C, thermal

desorption at 90 °C and mineralization desorption using CaO at 25 °C are summarized below. A new mechanism is proposed to explain carbamate increasing with significantly decreasing bicarbonate/carbonate at the early stage of mineralization desorption from our study.

The CO<sub>2</sub> absorption at 40 °C achieved the CO<sub>2</sub> loading from 0 to 0.76 mol/mol KG which had 0.33 mol/mol carbamate and 0.43 mol/mol bicarbonate/carbonate when the pH value was down from 13.93 to 8.40. Therefore, the CO<sub>2</sub> absorption efficiency is 76% which has 57% contributed by bicarbonate/carbonate and 43% by carbamate using KG as the absorbent. The CO<sub>2</sub> desorption efficiency by mineralization using CaO at 25 °C is higher than that by the thermal method at 90 °C (59% vs. 47%). Both methods have the same reduction in bicarbonate/carbonate but mineralization has more reduction in carbamate. This suggests that carbamate is more stable under heat than under mineralization. The CO<sub>2</sub> desorption efficiency in the CO<sub>2</sub>-rich KG solution is dominated by the reduction in bicarbonate/carbonate for both methods, about 90% for the thermal method and 75% for mineralization, different from what has been reported in literature using MEA as the absorbent. The carbamate content as a function of pH value is a convex curve having relatively the same maximum about 0.46–0.47 mol/mol KG, regardless of absorption or desorption processes. Bicarbonate/carbonate had the profile starting from 0 mol/mol to very low level and then a significant growth up to 0.43 mol/mol KG for absorption, but had the reverse curve stabilized at a very low level of 0.01–0.02 mol/mol KG for desorption, regardless of the thermal or mineralization method.

In the process of CO<sub>2</sub> absorption, the CO<sub>2</sub> was firstly directly absorbed by KG to form carbamate and protonated KG, before any bicarbonate/carbonate was formed. The literature has suggested primary amine reacted with dissolved CO<sub>2</sub> to form a zwitterion and the unstable zwitterion subsequently deprotonates to carbamate by giving a proton to a second amine molecule [60–62]. There was no evidence to prove the existence of the zwitterion in our study. Literature has not reported the bicarbonate/carbonate content still remained at a very low level during the early stage of absorption before the carbamate content reached its maximum as the pH value was continuously decreased. As the CO<sub>2</sub> absorption was approaching to the end, the carbamate content was decreased with increasing bicarbonate/carbonate. This mechanism has been proposed in literature by carbamate reacting with water to regenerate KG and produce bicarbonate.

At the beginning of thermal desorption, the loss of bicarbonate was

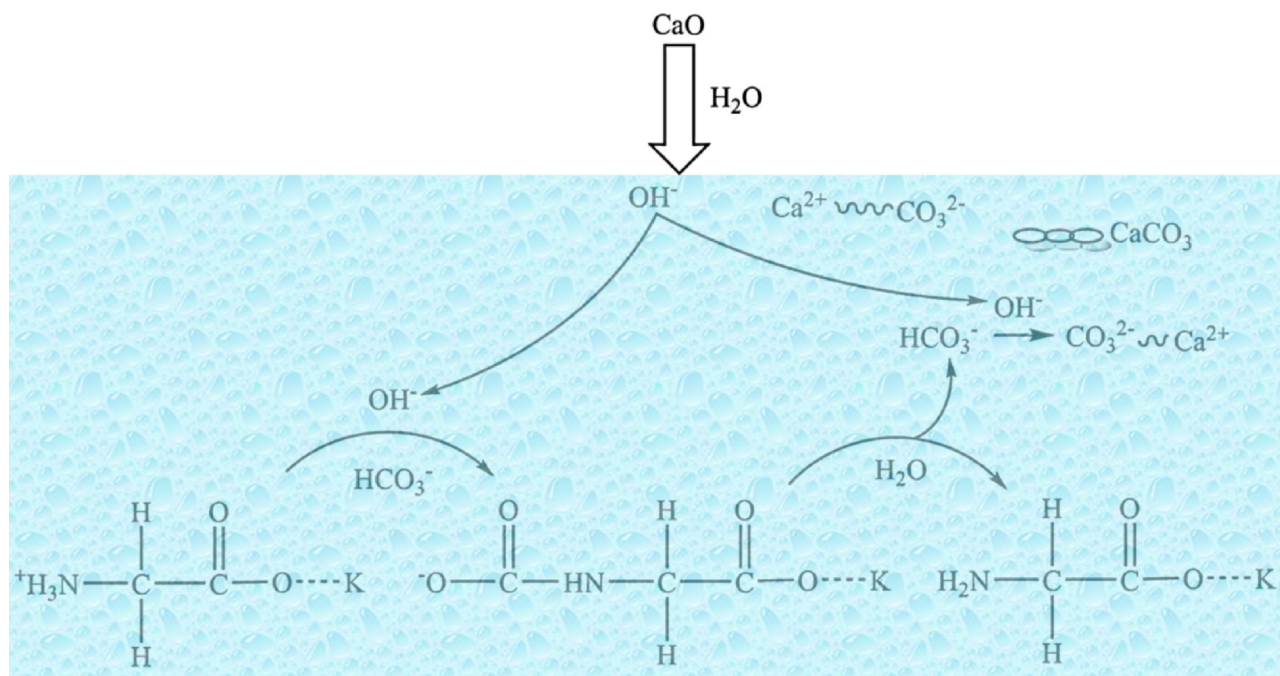


**Fig. 10.** Mechanisms of  $\text{CO}_2$ -rich KG solution for mineralization regeneration.

about twice of carbamate generation. This first thermal decomposition mechanism was proposed to have 2 mol bicarbonates reacting with 1 mol protonated KG to produce 1 mol carbamate and 1 mol  $\text{CO}_2$ . As the value of pH was continuously increased, the carbamate content was continuously increased to reach its maximum and remained relatively constant, suggesting that the proposed mechanism has been terminated. Then the reduction in bicarbonate/carbonate was due to the well-known thermal degradation mechanism by bicarbonate/carbonate reacting with protonated KG to regenerate KG and produce  $\text{CO}_2$ . As the thermal desorption was approaching to the end, the carbamate content was decreased with increasing pH, while bicarbonate/carbonate was reduced slightly and then remained relatively constant at a very low level. It had 1 mol carbamate and 1 mol protonated KG thermally degraded to generate 1 mol  $\text{CO}_2$  and 2 mol KG.

During the mineralization desorption in the  $\text{CO}_2$ -rich KG solution at 25 °C, the first mineralization mechanism is the well-known mechanism which has  $\text{CaO}$  dissolved in the alkaline solution to generate 1 mol  $\text{Ca}^{2+}$  and 2 mol  $\text{OH}^-$  and increase pH value. During the early mineralization, bicarbonate/carbonate was reduced in the amount twice of the increase in carbamate, similar to thermal degradation. A new mechanism was proposed to explain the increase in carbamate: 1 mol  $\text{HCO}_3^-$  and 1 mol  $\text{OH}^-$  reacting with 1 mol protonated KG to produce 1 mol carbamate. The other most common mineralization mechanism was also used to support the same reduction in bicarbonate/carbonate through  $\text{Ca}^{2+}$  reacting with  $\text{HCO}_3^-$  and  $\text{OH}^-$  to generate  $\text{CaCO}_3$  and  $\text{H}_2\text{O}$ . Both mechanisms were occurring simultaneously to explain loss of 2 mol bicarbonate/carbonate and increase of 1 mol carbamate. After carbamate reached its maximum value, carbamate was decreased but bicarbonate/carbonate was increased. The mechanism was similar to those proposed in the literature by carbamate reacting with water to regenerate KG and produce bicarbonate [27]. As the mineralization was approaching to the end, carbamate was continuously decreased while bicarbonate/carbonate remained relatively constant at a very low level, while pH was continuously increased. The mechanism was proposed to have  $\text{Ca}^{2+}$  reacting with carbamate and  $\text{OH}^-$  to regenerate KG and produce  $\text{CaCO}_3$ . Although many works had been carried out to find out the reaction mechanisms of  $\text{CO}_2$  absorption and desorption processes, little had been published on the entire mechanisms of the  $\text{CO}_2$ -rich solution for absorbent regeneration by mineralization. The reaction

pathways of mineralization for absorbent regeneration from protonated KG through carbamate to KG, differently from protonated KG to KG by the thermal method, have been confirmed by the  $^{13}\text{C}$  NMR spectroscopy in our study as shown in Fig. 10 in the  $\text{CO}_2$ -rich KG solution.

#### 4. Conclusion

In brief, potassium glycine as the absorbent shows the  $\text{CO}_2$  absorption efficiency up to 76% which has 57% due to the bicarbonate/carbonate formation and 43% due to the carbamate formation. Mineralization has a higher  $\text{CO}_2$  desorption efficiency of 59% than that of thermal desorption (47%). The results indicate that carbamate is less stable under mineralization than under heat, although both processes show the similar profiles as a function of pH value for carbamate and bicarbonate/carbonate.

In terms of reaction mechanisms, a new mechanism was proposed to explain 2 mol bicarbonate/carbonate reduction along with 1 mol carbamate increase during the early stage of  $\text{CO}_2$  desorption by the mineralization method. Our study clearly confirmed that carbamate formation started before the bicarbonate/carbonate formation at the beginning of the  $\text{CO}_2$  absorption experiment at 40 °C, reached its maximum and then decreased by being converted to bicarbonate and KG near the end of the absorption. The well-known desorption mechanisms of thermal degradation and carbonation (mineralization) for both bicarbonate/carbonate and carbamate have also been confirmed in this study.

#### Declaration of Competing Interest

The authors declare that they have no known competing financial interests or personal relationships that could have appeared to influence the work reported in this paper.

#### Acknowledgments

The authors are grateful for the funding from China Energy Investment Corporation (SHJT-16-24), and National Institute of Clean-and-Low-Carbon Energy (CF9300190043) to support this work.

## References

- [1] J.M. Matter, M. Stute, S.O. Snæbjørnsdóttir, E.H. Oelkers, S.R. Gislason, E.S. Aradottir, B. Sigfusson, I. Gunnarsson, H. Sigurdardóttir, E. Gunnlaugsson, G. Axelsson, H.A. Alfredsson, D. Wolff-Boenisch, K. Mesfin, D. Fernandez de la Reguera Taya, J. Hall, K. Dideriksen, W.S. Broecker, Rapid carbon mineralization for permanent disposal of anthropogenic carbon dioxide emissions, *Science* 352 (2016) 1312–1314.
- [2] R.A. Kerr, Climate change. Global warming is changing the world, *Science* 316 (2007) 188–190.
- [3] G.T. Rochelle, Amine scrubbing for CO<sub>2</sub> capture, *Science* 325 (2009) 1652–1654.
- [4] X. Yang, R.J. Rees, W. Conway, G. Puxty, Q. Yang, D.A. Winkler, Computational Modeling and Simulation of CO<sub>2</sub> Capture by Aqueous Amines, *Chem. Rev.* 117 (2017) 9524–9593.
- [5] J. Narku-Tetteh, P. Muchan, C. Saiwan, T. Supap, R. Idem, Selection of components for formulation of amine blends for post combustion CO<sub>2</sub> capture based on the side chain structure of primary, secondary and tertiary amines, *Chem. Eng. Sci.* 170 (2017) 542–560.
- [6] W. Conway, X. Wang, D. Fernandes, R. Burns, G. Lawrence, G. Puxty, M. Maeder, Toward the Understanding of Chemical Absorption Processes for Post-Combustion Capture of Carbon Dioxide: Electronic and Steric Considerations from the Kinetics of Reactions of CO<sub>2</sub>(aq) with Sterically hindered Amines, *Environ. Sci. Technol.* 47 (2013) 1163–1169.
- [7] P. Muchan, C. Saiwan, J. Narku-Tetteh, R. Idem, T. Supap, P. Tontiwachwuthikul, Screening tests of aqueous alkanolamine solutions based on primary, secondary, and tertiary structure for blended aqueous amine solution selection in post combustion CO<sub>2</sub> capture, *Chem. Eng. Sci.* 170 (2017) 574–582.
- [8] P.M.M. Blauwhoff, G. Versteeg, W. Van Swaaij, A Study on the Reaction Between CO<sub>2</sub> and Alkanolamines in Aqueous Solutions, *Chem. Eng. Sci.* 39 (1984) 207–225.
- [9] R.J. Hook, An Investigation of Some Sterically Hindered Amines as Potential Carbon Dioxide Scrubbing Compounds, *Ind. Eng. Chem. Res.* 36 (1997) 1779–1790.
- [10] A.F. Portugal, P.W.J. Derkx, G.F. Versteeg, F.D. Magalhães, A. Mendes, Characterization of potassium glycinate for carbon dioxide absorption purposes, *Chem. Eng. Sci.* 62 (2007) 6534–6547.
- [11] A.F. Portugal, J.M. Sousa, F.D. Magalhães, A. Mendes, Solubility of carbon dioxide in aqueous solutions of amino acid salts, *Chem. Eng. Sci.* 64 (2009) 1993–2002.
- [12] P.D. Vaidya, P. Kondu, M. Vaidyanathan, E.Y. Kenig, Kinetics of Carbon Dioxide Removal by Aqueous Alkaline Amino Acid Salts, *Ind. Eng. Chem. Res.* 49 (2010) 11067–11072.
- [13] S. Lee, H.-J. Song, S. Maken, J.-W. Park, Kinetics of CO<sub>2</sub> Absorption in Aqueous Sodium Glycinate Solutions, *Ind. Eng. Chem. Res.* 46 (2007) 1578–1583.
- [14] P.S. Kumar, J.A. Hogendoorn, G.F. Versteeg, P.H.M. Feron, Kinetics of the reaction of CO<sub>2</sub> with aqueous potassium salt of taurine and glycine, *AIChE J.* 49 (2003) 203–213.
- [15] D.E. Penny, T.J. Ritter, Kinetic study of the reaction between carbon dioxide and primary amines, *J. Chem. Soc., Faraday Trans. 1* 79 (1983) 2103.
- [16] G.S. Goff, G.T. Rochelle, Oxidative degradation of monoethanolamine in CO<sub>2</sub> capture: O<sub>2</sub> Mass transfer, *Greenhouse Gas Control Technol.* 7 (2005) 1831–1834.
- [17] G. Versteeg, J. Niederer, E. Hamborg, Dissociation Constants and Thermodynamic Properties of Amino Acids Used in CO<sub>2</sub> Absorption from (293 to 353) K, *J. Chem. Eng. Data* 52 (2007) 2491–2502.
- [18] U. Aronu, A. Ciftja, I. Kim, A. Hartono, Understanding Precipitation in Amino Acid Salt systems at Process Conditions, *Energy Procedia* 37 (2013) 233–240.
- [19] U. Aronu, H. Svendsen, K. Hoff, Investigation of amine amino acid salts for carbon dioxide absorption, *Int. J. Greenhouse Gas Control* 4 (2010) 771–775.
- [20] D. Guo, H. Thee, C.Y. Tan, J. Chen, W. Fei, S. Kentish, G.W. Stevens, G. da Silva, Amino Acids as Carbon Capture Solvents: Chemical Kinetics and Mechanism of the Glycine + CO<sub>2</sub> Reaction, *Energy Fuels* 27 (2013) 3898–3904.
- [21] H. Thee, N.J. Nicholas, K.H. Smith, G. da Silva, S.E. Kentish, G.W. Stevens, A kinetic study of CO<sub>2</sub> capture with potassium carbonate solutions promoted with various amino acids: Glycine, sarcosine and proline, *Int. J. Greenhouse Gas Control* 20 (2014) 212–222.
- [22] E. Sanchez-Fernandez, K. Heffernan, L.V. van der Ham, M.J.G. Linders, E. Eggink, F.N.H. Schrama, D.W.F. Brilman, E.L.V. Goetheer, T.J.H. Vlugt, Conceptual Design of a Novel CO<sub>2</sub> Capture Process Based on Precipitating Amino Acid Solvents, *Ind. Eng. Chem. Res.* 52 (2013) 12223–12235.
- [23] E. Sanchez-Fernandez, F.d.M.K.L.M.E. New Process Concepts for CO<sub>2</sub> Capture based on Precipitating Amino Acids, *Energy Procedia* 37 (2013) 1160–1171.
- [24] M.E. Majchrowicz, D.W.F. Brilman, M.J. Groeneveld, Precipitation regime for selected amino acid salts for CO<sub>2</sub> capture from flue gases, *Energy Procedia* 1 (2009) 979–984.
- [25] E. Sanchez-Fernandez, K. Heffernan, L. van der Ham, M.J.G. Linders, D.W.F. Brilman, E.L.V. Goetheer, T.J.H. Vlugt, Analysis of Process Configurations for CO<sub>2</sub> Capture by Precipitating Amino Acid Solvents, *Ind. Eng. Chem. Res.* 53 (2014) 2348–2361.
- [26] H.-J. Song, S. Lee, K. Park, J. Lee, D. Spah, J.-W. Park, T. Filburn, Simplified Estimation of Regeneration Energy of 30 wt % Sodium Glycinate Solution for Carbon Dioxide Absorption, *Industrial & Engineering Chemistry Research - Ind. Eng. Chem. Res.* 47 (2008) 9925–9930.
- [27] G. Gadikota, Multiphase carbon mineralization for the reactive separation of CO<sub>2</sub> and directed synthesis of H<sub>2</sub>, *Nat. Rev. Chem.* 4 (2020) 78–89.
- [28] A. García-Abuín, D. Gómez-Díaz, J.M. Navaza, New processes for amine regeneration, *Fuel* 135 (2014) 191–197.
- [29] D. Gómez-Díaz, Use of New Regeneration Processes for Thermolabile Amines, *Int. J. Chem. Reactor Eng.* 14 (2016) 533–537.
- [30] J. Bentes, A. García-Abuín, A.G. Gomes, D. Gómez-Díaz, J.M. Navaza, A. Rumbo, CO<sub>2</sub> chemical absorption in 3-amino-1-propanol aqueous solutions in BC reactor, *Fuel Process. Technol.* 137 (2015) 179–185.
- [31] M. Castro, D. Gómez-Díaz, J.M. Navaza, Carbon dioxide chemical absorption using methylpiperidines aqueous solutions, *Fuel* 197 (2017) 194–200.
- [32] M. Carrera, D. Gómez-Díaz, J.M. Navaza, Switchable hydrophilicity solvents for carbon dioxide chemical absorption, *J. Ind. Eng. Chem.* 59 (2018) 304–309.
- [33] L. Ji, H. Yu, K.K. Li, B. Yu, M. Grigore, Q. Yang, X. Wang, Z. Chen, M. Zeng, S. Zhao, Integrated absorption-mineralisation for low-energy CO<sub>2</sub> capture and sequestration, *Appl. Energy* 225 (2018) 356–366.
- [34] L. Ji, H. Yu, B. Yu, K. Jiang, M. Grigore, X. Wang, S. Zhao, K. Li, Integrated absorption – mineralisation for energy-efficient CO<sub>2</sub> sequestration: Reaction mechanism and feasibility of using fly ash as a feedstock, *Chem. Eng. J.* 352 (2018) 151–162.
- [35] S. Bishnoi, G. Rochelle, Thermodynamics of Piperazine/Methylidiethanolamine/Water/Carbon Dioxide, *Ind. Eng. Chem. Res.– Ind. Eng. Chem. Res.* 41 (2002) 604–612.
- [36] J. Cullinane, G. Rochelle, Thermodynamics of aqueous potassium carbonate, piperazine, and carbon dioxide, *Fluid Phase Equilib.* 227 (2005) 197–213.
- [37] J. Jakobsen, J. Krane, H. Svendsen, Liquid-Phase Composition Determination in CO<sub>2</sub> – H<sub>2</sub>O – Alkanolamine Systems: An NMR Study, *Ind. Eng. Chem. Res.– Ind. Eng. Chem. Res.* 44 (2005) 9894–9903.
- [38] S. Bishnoi, G. Rochelle, Absorption of carbon dioxide into aqueous piperazine: Reaction kinetics, mass transfer and solubility, *Chem. Eng. Sci.* 55 (2000) 5531–5543.
- [39] A.K. Chakraborty, G. Astarita, K.B. Bischoff, CO<sub>2</sub> Absorption in Aqueous Solutions of Hindered Amines, *Chem. Eng. Sci.* 41 (1986) 997–1003.
- [40] J.-Y. Park, S. Yoon, H. Lee, Effect of Steric Hindrance on Carbon Dioxide Absorption into New Amine Solutions: Thermodynamic and Spectroscopic Verification through Solubility and NMR Analysis, *Environ. Sci. Technol.* 37 (2003) 1670–1675.
- [41] A. Hartono, U. Aronu, H. Svendsen, Liquid Speciation Study in Amine Amino Acid Salts for CO<sub>2</sub> Absorbent with <sup>13</sup>C-NMR, *Energy Procedia* 4 (2011) 209–215.
- [42] A. Hartono, E. Silva, H. Grasdalen, H. Svendsen, Qualitative determination of species in DETA-H<sub>2</sub>O-CO<sub>2</sub> system using <sup>13</sup>C NMR spectra, *Ind. Eng. Chem. Res.– Ind. Eng. Chem. Res.* 46 (2007) 249–254.
- [43] B. Lv, B.-S. Guo, Z. Zhou, G.-H. Jing, Mechanisms of CO<sub>2</sub> Capture into Monoethanolamine Solution with Different CO<sub>2</sub> Loading during the Absorption/Desorption Processes, *Environmental Science & Technology* 49 (2015) 10728–10735.
- [44] N. McCann, D. Phan, M. Maeder, A systematic investigation of carbamate stability constants by <sup>1</sup>H NMR, *Int. J. Greenhouse Gas Control* 5 (2011) 396–400.
- [45] J.H. Choi, S. Oh, Y. Yoon, S. Jeong, K. Jang, S. Nam, A Study of Species Formation of Aqueous Tertiary and Hindered Amines Using Quantitative <sup>13</sup>C NMR Spectroscopy, *Journal of Industrial and Engineering Chemistry – J. Ind. Eng. Chem.* 18 (2012) 568–573.
- [46] F. Barzaghi, F. Mani, M. Peruzzini, A <sup>1</sup>H NMR investigation of CO<sub>2</sub> absorption and desorption in aqueous 2,2'-iminodiethanol and N-methyl-2,2'-iminodiethanol, *Int. J. Greenhouse Gas Control* 5 (2011) 448–456.
- [47] C. Guo, S. Chen, Y. Zhang, A <sup>13</sup>C NMR study of carbon dioxide absorption and desorption in pure and blended 2-(2-aminoethylamine)ethanol (AEEA) and 2-amino-2-methyl-1-propanol (AMP) solutions, *Int. J. Greenhouse Gas Control* 28 (2014) 88–95.
- [48] A. Ciftja, A. Hartono, E. Silva, H. Svendsen, Study on carbamate stability in the AMP/CO<sub>2</sub>/H<sub>2</sub>O system from <sup>13</sup>C-NMR spectroscopy, *Energy Procedia* 4 (2011) 614–620.
- [49] M. Ballard, M. Bown, S. James, Q. Yang, NMR studies of mixed amines, *Energy Procedia* 4 (2011) 291–298.
- [50] F. Barzaghi, F. Mani, M. Peruzzini, Continuous cycles of CO<sub>2</sub> absorption and amine regeneration with aqueous alkanolamines: A comparison of the efficiency between pure and blended DEA, MDEA and AMP solutions by <sup>13</sup>C NMR spectroscopy, *Energy Environ. Sci.* 3 (2010) 772–779.
- [51] C. Guo, S. Chen, S. Chen, Y. Zhang, Quantitative analysis on CO<sub>2</sub> absorption and desorption in monoethanolamine (MEA) solution by using <sup>13</sup>C NMR, *Chem. Indust. Eng. Progr.* 33 (2014) 3101–3106.
- [52] S. Kim, Y. Seo, Semiclathrate-based CO<sub>2</sub> capture from flue gas mixtures: An experimental approach with thermodynamic and Raman spectroscopic analyses, *Appl. Energy* 154 (2015) 987–994.
- [53] D. Peltzer, J. Múnera, L. Cornaglia, Operando Raman spectroscopic studies of lithium zirconates during CO<sub>2</sub> capture at high temperature, *RSC Adv.* 6 (2016) 8222–8231.
- [54] B. Yu, H. Yu, K. Li, Q. Yang, R. Zhang, L. Li, Z. Chen, Characterisation and kinetic study of carbon dioxide absorption by an aqueous diamine solution, *Appl. Energy* 208 (2017) 1308–1317.
- [55] G. Richner, G. Puxty, Assessing the Chemical Speciation during CO<sub>2</sub> Absorption by Aqueous Amines Using in Situ FTIR, *Ind. Eng. Chem. Res.* 51 (2012) 14317–14324.
- [56] K. Robinson, A. McCluskey, M.I. Attalla, An FTIR Spectroscopic Study on the Effect of Molecular Structural Variations on the CO<sub>2</sub> Absorption Characteristics of Heterocyclic Amines, Part II, *Chempysche: A Eur. J. Chem. Phys. Phys. Chem.* 12 (2011) 1088–1099.
- [57] K. Robinson, A. McCluskey, M.I. Attalla, An ATR-FTIR Study on the Effect of Molecular Structural Variations on the CO<sub>2</sub> Absorption Characteristics of Heterocyclic Amines, Part II, *Chempysche: A Eur. J. Chem. Phys. Phys. Chem.* 13 (2012) 2331–2341.
- [58] Y. Li, H.P. Wang, C.-Y. Liao, X. Zhao, T.-L. Hsiung, S.-H. Liu, S.-G. Chang, Dual Alkali Solvent System for CO<sub>2</sub> Capture from Flue Gas, *Environ. Sci. Technol.* 51 (2017) 8824–8831.

- [59] L. Ji, H. Yu, X. Wang, M. Grigore, D. French, Y.M. Gözükara, J. Yu, M. Zeng, CO<sub>2</sub> sequestration by direct mineralisation using fly ash from Chinese Shenfu coal, *Fuel Process. Technol.* 156 (2017) 429–437.
- [60] J. Xiao, S. Sitamraju, M.J. Janik, CO<sub>2</sub> adsorption thermodynamics over N-substituted/grafted graphanes: a DFT study, *Langmuir* 30 (2014) 1837–1844.
- [61] S. Gangarapu, A.T.M. Marcelis, H. Zuilhof, Improving the Capture of CO<sub>2</sub> by Substituted Monoethanolamines: Electronic Effects of Fluorine and Methyl Substituents, *Chemphyschem: A Eur. J. Chem. Phys. Phys. Chem.* 13 (2012) 3973–3980.
- [62] Q. Yang, G. Puxty, S. James, M. Bown, P. Feron, W. Conway, Toward Intelligent CO<sub>2</sub> Capture Solvent Design through Experimental Solvent Development and Amine Synthesis, *Energy Fuels* 30 (2016) 7503–7510.